Direct Analysis of the Ion-Hopping Process Associated with the α-Relaxation in Perfluorosulfonate Ionomers Using Quasielastic Neutron Scattering[†]

Kirt A. Page,*,‡ Jong Keun Park,§ Robert B. Moore,§ and Victoria Garcia Sakai‖,⊥,#

Polymers Division, National Institute of Standards and Technology, Gaithersburg, Maryland 20899, Department of Chemistry, Virginia Polytechnic Institute and State University, Blacksburg, Virginia 24061, NIST Center for Neutron Research, National Institute of Standards and Technology, Gaithersburg, Maryland 20899, and Department of Materials Science and Engineering, University of Maryland, College Park, Maryland 20742

ABSTRACT: This work demonstrates the ability of quasielastic neutron scattering (QENS) to measure the dynamics associated with counterions in perfluorosulfonate ionomers (PFSIs). PFSI membranes were prepared by neutralizing with hydrogenated alkyl ammonium counterions. Counterion dynamics were measured using the High-Flux Backscattering Spectrometer at the National Institute of Standards and Technology (NIST) Center for Neutron Research (NCNR). Long-range mobility of the counterions was closely linked with the α-relaxation in these materials measured by dynamic mechanical analysis (DMA). The counterion motions in the membrane were found to follow a mechanism of random jump-diffusion within a confined spatial region with diffusion coefficients on the order of 10^{-7} cm^2 s^{-1}. These data are presented along with variable temperature X-ray scattering investigations of the melting behavior of these materials. Altogether, the data presented here show the link between the onset of long-range counterion mobility and the mechanical properties of these materials. These data provide further fundamental understanding of the link between electrostatic interactions and dynamics in PFSI materials.

Introduction

Ionomers are an interesting class of polymeric materials that contain ionic comonomer units distributed along the polymer backbone and have been the focus of many studies over the last several decades.[1–17] The physical properties of these materials are dictated by the Coulombic interactions between the ion-pairs along the backbone. These electrostatic interactions lead to the formation of stable ionic associations that behave in many ways as cross-links. In particular, the relaxation behavior of these materials is greatly affected by the associations, and the resulting aggregates (multiplets), and has been the focus of several rheological studies.[11–14,16,17] Several studies have shown that the rheological behavior of these materials can be altered simply by changing the degree of neutralization or through the choice of counterion, factors that can be expected to influence the strength of the associations.[7] In particular, and pertinent to later discussion, early patent literature describes the neutralization of ionomers with alkyl ammonium ions and subsequent changes in the rheological properties.[18] In addition, Weiss et al.[15] observed a decrease in the viscosity of alkylamine neutralized polystyrene ionomers with an increase in the bulkiness of the counterion and found that electrostatic interactions predominate for smaller counterions, while plasticization (increase in the segmental dynamics) is more important as the counterion becomes sufficiently bulky. These, and other studies,

show that by changing the overall number and strength of the electrostatic interactions, a large degree of control can be exerted over the relaxation processes in these materials.

Although it is beyond the scope of this discussion, there have been several investigations of the relaxation behavior of ion containing polymers.[1,10] In short, two "glass transition" temperatures (T_g) have been reported for ion containing polymers: one attributed to the T_g of the "matrix" chains removed from the ionic aggregates and the other attributed to the T_g of the "cluster" domains, or chains in the vicinity of an ionic aggregate that have a restricted mobility due to decreased conformational entropy. Our work has shown that for perfluorosulfonate ionomers (PFSIs) this description of the relaxation processes is not entirely accurate.[19,20] However, there are similarities in our description of the relaxations in PFSIs and the classical ionomer description.

The two predominant relaxation processes governing the melt rheological behavior of ionomers, in general, are (1) the terminal relaxation time of the polymer chains and (2) the average lifetime of the ionic associations.[13] Ultimately, the terminal relaxation time is dictated by the time that an ion pair resides in an aggregate before "hopping" to another aggregation site. This process has been termed "ion-hopping", and τ is the ion-hopping time.[2,4,9,11–14,21] The relative time scale of these two processes has been studied using rheology and cation diffusion measurements. The onset of this ion hopping process has been experimentally observed for both styrenecarboxylates and styrenesulfonates.[9,21,22] Ion-hopping has been identified as a principle phenomenon in the mechanism for the cluster "glass transition", or α-relaxation process, for these materials. Essentially, the presence of appreciable ion-hopping means the ionic aggregates are dynamic and the rigidity of the system is reduced because of the labile nature of these associations.[1] The concept of a temperature at which the electrostatic cross-links (i.e., multiplets) become thermodynamically unstable was proposed by Eisenberg in a theoretical description of clustering in ionomers in 1970.[3] The "ion-hopping temperature", of

---

[†] Reported data error bars and value uncertainties represent one standard deviation as the estimated standard uncertainty of the measurements and the fits, respectively.

* To whom all correspondence should be addressed. E-mail: kirt.page@nist.gov.

‡ Polymers Division, National Institute of Standards and Technology.

§ Department of Chemistry, Virginia Polytechnic Institute and State University.

‖ Current address: ISIS Facility, Rutherford Appleton Laboratory, Chilton, Didcot, OX11 0QX, U.K.

⊥ NIST Center for Neutron Research, National Institute of Standards and Technology.

Department of Materials Science and Engineering, University of Maryland.

Eisenberg's, is defined as the temperature at which the multiplet becomes thermodynamically unstable and the elastic forces of the chain are balanced with the electrostatic forces of the aggregates.[3] Our previous work has drawn upon the concept of ion-hopping to explain the molecular origins of the relaxation processes in PFSIs.[19,20] It should be clarified that we are careful not to definitively assign the α-relaxation to a pure glass transition temperature, but rather to a transition from a state exhibiting static electrostatic cross-links to a state exhibiting dynamic electrostatic cross-links brought about by the onset of ion-hopping. Furthermore, both the α-relaxation and the ion-hopping phenomenon are recognized to be frequency dependent, dynamic processes.

Recent simulations of ionomer self-assembly by Kumar and co-workers[23] provide some basic insights into the nature of these fluids. Upon cooling, there is first a transition where the counterions pair with the ions on the chain backbone to form small ion-multiplet structures that remain quite mobile. The character of these ion pairs in "primitive model" ionic fluids has been shown to depend on ion valence and ion size asymmetry,[24,25] forming dipolar, or multiple, low energy structures depending on these asymmetry factors. The long-range interactions of the small ion-multiplet structures lead to the supermolecular assembly of the small ion-multiplets (ribbon-like structures in the simulations of Kumar and co-workers) in a well-defined order−disorder transition upon further cooling characterized by a maximum in the specific heat and a sharp drop in the mobility of counterions that have been incorporated into the self-assembled structures. Kumar and co-workers suggest that this self-assembly transition can be identified with the "cluster T_g" of Eisenberg.[3,4,23] The second, lower T_g, is naturally attributed to the conventional T_g of the polymeric structures with the large-scale supermolecularly assembled ionomer multiplet structures. The description put forth by the simulations of Kumar et al.[23] is congruent with earlier descriptions of the relaxation processes for PFSIs. It is apparent that the "self-assembly" of the ion pairs into supermolecular structures that they observe upon cooling corresponds to the same process involved in destabilization of the electrostatic network upon heating described in earlier work.

Nafion is a widely examined PFSI and the focus of our work.[26]

The perfluoroether side-chains containing the ionic, sulfonate groups have been shown to organize into aggregates, thus leading to a nanophase-separated morphology where the ionic domains, termed clusters, are distributed throughout the nonpolar poly(tetrafluoroethylene) (PTFE) matrix. This morphology gives a characteristic scattering peak in small-angle X-ray and neutron scattering centered at $Q = 0.20$ Å^{-1} ($Q = 2\pi/d$, where d is the length scale of motion).[26] The membranes used in this study have been neutralized with tetramethylammonium (TMA$^+$) and tetrabutyl ammonium (TBA$^+$) counterions according to previously published methods.[19,20] The size, or polarizability, of the counterion influences the strength of the electrostatic network, thus changing the chain dynamics and, in turn, the mechanical properties.[19,20]

Our earlier studies of these materials correlating dynamic mechanical analysis (DMA) with a variety of other techniques show that the α-relaxation of these materials is due to the onset of long-range mobility of both the main- and side-chains, which

is facilitated by a profound weakening of the electrostatic interactions within the ionic aggregates. At temperatures in the vicinity of the α-relaxation (T_α), a significant destabilization of the electrostatic network may be observed, which results in the activation of a *dynamic* network facilitated through the ion-hopping process described earlier. In contrast, the β-relaxation (T_β) was associated with the onset of segmental motions (principally backbone motions) within the framework of a *static* physically cross-linked network of chains.[19,20]

The present work uses quasielastic neutron scattering (QENS) to investigate the correlations between counterion dynamics and the bulk mechanical relaxations in alkyl ammonium neutralized PFSIs in order to obtain a better understanding of the physical basis of the relaxation processes in these materials. QENS provides a direct measure of counterion dynamics, making it possible to calculate time-scales associated with the motions of the ions and ion diffusion coefficients for temperatures above the α-relaxation. QENS measures the dynamic structure factor in the frequency domain, thus providing information about the motions of atoms, or molecules, on a time scale of $10^{-8} - 10^{-13}$ s. QENS is sensitive to the motion of hydrogen atoms, which have a significantly larger incoherent scattering length than other atoms. In the systems presented here, only the counterions contain hydrogen, thus allowing us to isolate the dynamics of the counterions. We use QENS to study the counterion dynamics, and thus directly confirm and characterize the ion-hopping process.

Experimental Section

Materials. Nafion 117 (1100 EW, sulfonic acid form) films were obtained from E. I. du Pont de Nemours & Co. The tetramethyl- (TMA$^+$), tetraethyl- (TEA$^+$), and tetrabutylammonium (TBA$^+$) counterions were obtained from Aldrich in the form of hydroxides dissolved in either water or methanol. All other reagents were obtained from Aldrich and used without further purification.

PFSI Sample Preparation. The PFSI membranes were cleaned by refluxing in 4 mol/L methanolic H$_2$SO$_4$ for ca. 12 h. These H$^+$-form membranes were then washed with deionized (DI) water to remove excess acid. The TMA$^+$, TEA$^+$, and TBA$^+$ form samples were prepared by soaking the H$^+$-form membranes in a 5 M excess of solutions of the appropriate alkylammonium hydroxide. The neutralized membranes were then thoroughly rinsed of excess alkylammonium hydroxide and dried in a vacuum oven at 70 °C, overnight.

Quasielastic Neutron Scattering. The QENS experiments were performed on the High-Flux Backscattering Spectrometer (HFBS)[27] at the National Institute of Standards and Technology (NIST) Center for Neutron Research (NCNR). Films of 145 μm thickness (5.5 cm × 8 cm), used to achieve ~90% neutron transmission through the sample and avoid multiple scattering, were loaded into annular, thin-walled (500 μm) aluminum cells and mounted to a closed-cycle refrigerator unit. Initial temperature scans were performed with the instrument in the so-called fixed window mode, where only the elastic scattering is measured, over a temperature range from −223 to +277 °C, at a heating rate of 1 °C/min and over a momentum transfer (or scattering vector, Q) range from 0.25 to 1.75 Å^{-1}. The raw data were normalized to the beam monitor. In general, such scans are comparable to thermal techniques such as differential scanning calorimetry (DSC) and clearly show relaxations in the system. Further information regarding the dynamics of the counterions was obtained from measuring the dynamic structure factor, $S(Q,\omega)$, at different temperatures using an energy range ±17 μeV (resolution of 0.85 μeV) and over a Q range 0.25−1.75 Å^{-1}. The data were reduced by normalizing intensity of beam monitor and corrected for detector efficiency. The instrument resolution function was measured by performing a dynamic scan on the sample at −233 °C. At this temperature, we assume that all motions are "frozen" and that the scattering is purely elastic. The data reduction and the analysis, including peak deconvolution were carried out
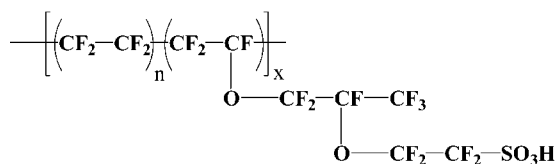
using DAVE [Data Analysis and Visualization Environment], a software package developed at the NCNR.[28]

Small-Angle X-ray and Neutron Scattering (SAXS/SANS). Variable temperature (VT), time-resolved small-angle X-ray scattering was performed at the Brookhaven National Laboratory on the Advanced Polymer Beamline (X27C) at the National Synchrotron Light Source. The incident X-ray beam was tuned to a wavelength of 0.1366 nm and the sample to detector distance was 85 cm. The two-dimensional scattering images were recorded using a Mar CCD camera with an intensity uncertainty on the order of 2%. The Nafion samples were heated in a sample chamber in the X-ray beam at a heating rate of 5 °C/min with an uncertainty of $\pm$ 1 °C while acquisition times were kept to 1 min and data were recorded from 50 to 300 °C. Intensity versus pixel data were obtained from the integration of the 2-D images using the POLAR software developed by Stonybrook Technology and Applied Research, Inc. The relationship between pixel and the momentum transfer vector Q was determined by calibrating the scattering data with a silver behenate standard. All scattering intensities were corrected for transmission, incident beam flux, and background scatter due to air and Kapton windows.

The SANS measurements were carried out on the NG7 beamline at the NCNR. The NG7 beamline includes a high-resolution 2D neutron detector (65×65) cm^2 and focusing refractive lenses. The instrument employs a mechanical velocity selector as a monochromator and a circular pinhole collimator. The SANS intensity, I, was recorded as a function of the magnitude of the scattering vector Q ($Q = 4\pi \sin(\theta/2)/\lambda$, where θ is the scattering angle and λ is the neutron wavelength, equal to 6 Å) and corrected for film thickness and background. The detector angle was set at 0°, and the sample-to-detector distance was set to 1 m, 4.5 m, and 13 m to cover the Q range 0.003−0.6 Å^{-1}. These settings enable one to probe structural features in materials ranging from approximately 10 to 2000 Å. The intensity was corrected for background scatter, sample thickness, and detector dark current using software developed at the NCNR.[29]

Wide-Angle X-ray Diffraction (WAXD). Synchrotron wide-angle X-ray diffraction (WAXD) was performed at the Argonne National Laboratory on the DND-CAT (5-ID) beamline at the Advanced Photon Source. The wavelength of the incident X-ray was 0.82656 Å and the sample-to-detector distance was 236 mm. The samples were heated from 50 to 300 °C using a Linkam heating stage (THMS600) at a heating rate of 5 °C/min (temperature stability <0.1 °C) and two-dimensional scattering patterns were recorded every 10 °C using a Roper Scientific detector. All scattering intensities were corrected for incident beam flux, background scatter due to air, and thickness of each sample. The scattering profiles are displayed as absolute intensity (cm^{-1}) as a function of the scattering vector, Q.

Results and Discussion

SAXS/WAXD/SANS. *Variable Temperature SAXS/WAXD.* To ensure that we can eliminate potential contributions from melting of PFSI crystallites on the α-relaxation, we have investigated the effect of counterion on the melting behavior and, thus the α-relaxation in these systems. In order to determine whether changes in the α-relaxation temperature as a function of counterion are related to melting of the Nafion crystallites, VT-SAXS and VT-WAXD experiments were performed. The VT-SAXS profiles for TMA$^+$ and TBA$^+$ Nafion can be seen in Figure 1, parts A and B. The peak at approximately 0.045 Å^{-1} arises from the long-range correlations between the Nafion crystallites. One can see that the long-period peak, due to the crystallites, begins to decrease in intensity at temperatures between 243 and 248 °C for TMA$^+$ and between 237 and 248 °C for TBA$^+$ Nafion. This demonstrates that melting is only slightly affected by the choice of the counterion. Further confirmation of this can be found in the VT-WAXD. Parts A and B of Figure 2 show the WAXD patterns for TMA$^+$ and TBA$^+$ Nafion over the temperature range of 220 to 300 °C.
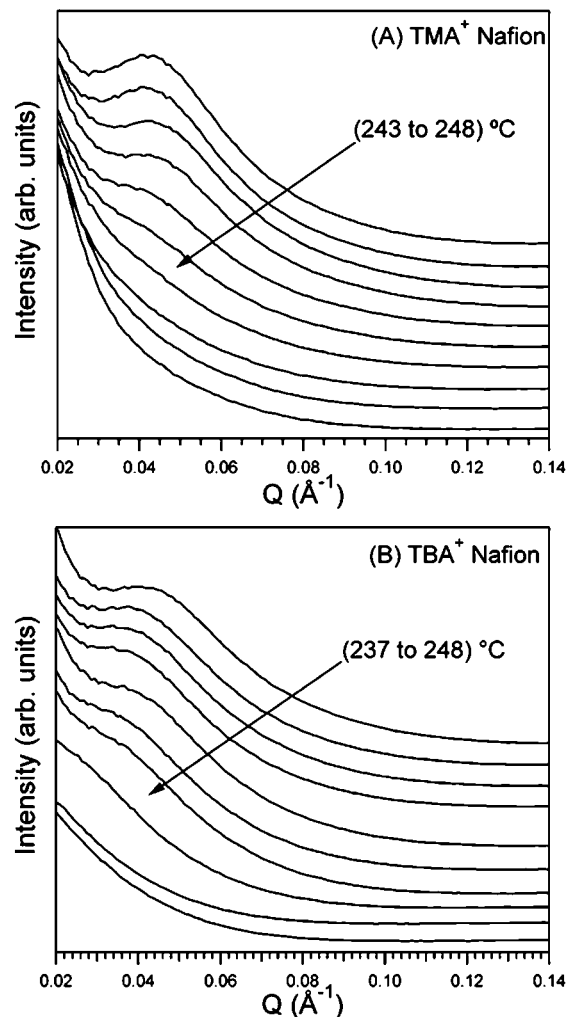
Figure 1. Variable temperature SAXS profiles for (A) TMA$^+$ and (B) TBA$^+$ Nafion.

There are many features in the WAXD, however, discussion will be limited to the peak at approximately 1.2 Å^{-1}, which is due to the (100) plane of the Nafion crystallites. Again, these data show that the crystalline peak decreases (due to melting) in an identical fashion for both counterion types. However, unlike the counterion independent melting, it has been demonstrated[19,20,30] that the α-relaxation temperature can be changed by as much as 137 °C just by changing the counterion from TMA$^+$ to TBA$^+$. This is clear evidence that the presence of crystallinity has little, if any, effect of the α-relaxation for these materials.

SANS. In order to gain insight into the dynamics as measured by QENS, it is necessary to measure the neutron scattering behavior of these materials. The SANS data for both TMA$^+$ and TBA$^+$ Nafion are shown in Figure 3. As discussed earlier, the peak at approximately 0.2 Å^{-1} is due to the interaggregate spacing. Although there is still much debate over the exact morphological structures giving rise to this peak, this discussion is not in the scope of this publication and it is important only that this peak is, indeed, due to correlations between domains containing the counterions in the system. The line at 0.25 Å^{-1} shows the lowest Q value accessible by HFBS at NIST. While this Q value is not sufficiently low enough to match the exact length scale associated with the aggregates, there is still enough intensity due to scattering from the ionomer structure to describe the dynamics of the counterions on a length scale close to that of the interaggregate spacing.
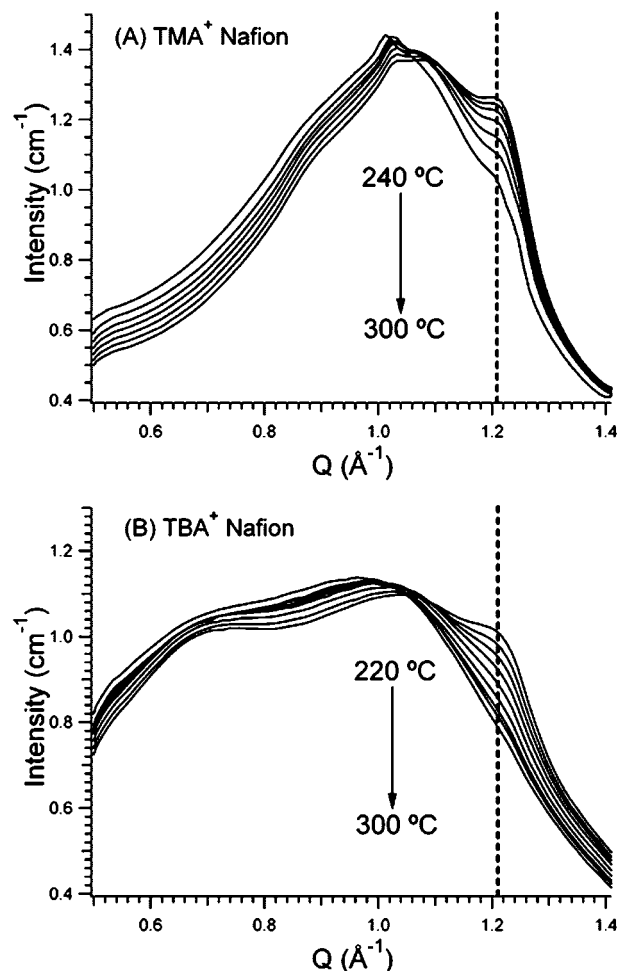
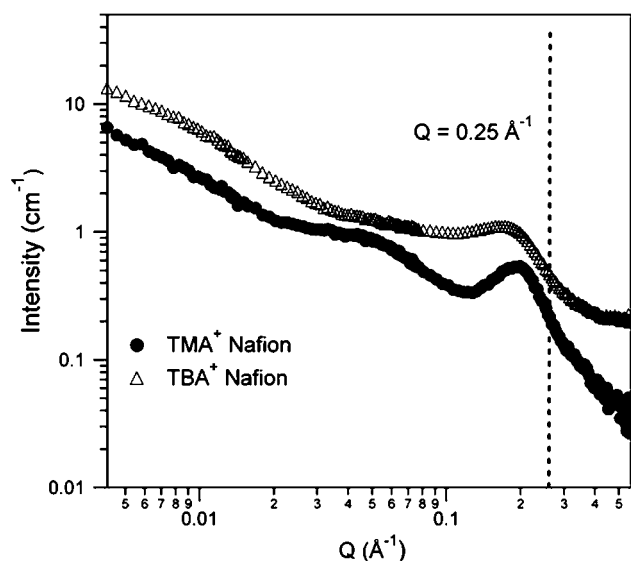**Figure 2.** Variable temperature WAXD profiles for (A) TMA$^+$ and (B) TBA$^+$ Nafion.

Figure 3. SANS profiles for (○) TMA$^+$ and (□) TBA$^+$ Nafion. The peak at ca. 0.2 Å^{-1} is the ionomer peak. The dotted line represents the Q value, 0.25 Å^{-1}, at which the QENS fixed-window scans were taken.

Quasielastic Neutron Scattering (QENS). *Variable Temperature Elastic Scattering.* The temperature-dependent elastic scattering at wavevectors of $Q = 0.25$ Å^{-1} and $Q = 0.99$ Å^{-1} for TMA$^+$, TEA$^+$, and TBA$^+$ Nafion can be seen in Figure 4, parts A and B. For $Q = 0.25$ Å^{-1}, Figure 4A, the elastic
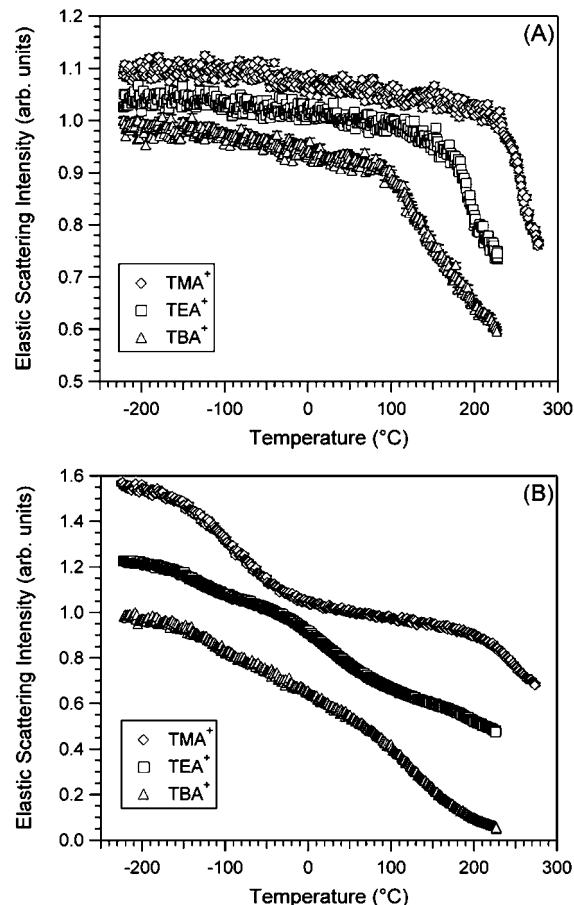
Figure 4. Fixed-window, elastic scans for (◇)TMA$^+$, (□)TEA$^+$, and (△)TBA$^+$ Nafion at (A) $Q = 0.25$ Å^{-1} and (B) $Q = 0.99$ Å^{-1}.

Table 1. Comparison of Mechanical Data from References 19 and 20 with the QENS Measurements

	DMA		
counterion form	T_α (°C)	T_β (°C)	QENS (°C)
TMA$^+$	237	133	234
TEA$^+$	160	111	167
TBA$^+$	100	72	97

scattering from each sample exhibits a distinct drop in intensity, which is attributed to the onset of mobility of the counterions having motions on a length scale of approximately 25 Å. The transition observed from the fixed-window data was determined from the intersection of two lines taken on each side of the transition. The results of this estimation are given in Table 1 along with data from dynamic mechanical analysis (DMA) adopted from our previous work.[19,20] The most striking feature of this data is the excellent correlation between the transition temperature in the elastic scattering intensity and the α-relaxation temperature (T_α) obtained by DMA. These data give unequivocal evidence that the α-relaxation is linked with the onset of "long-range" mobility of the counter-ions, thus lending support to our previous assignment of the molecular origins of the α-relaxation to an ion-hopping transition.[19,20]

It is interesting that the fast relaxations (ca. 10^8 Hz) measured by QENS are comparable to relaxations measured by other techniques such as DMA, DSC and dielectric measurements, which probe relaxations on a much longer time scale. However, there is sufficient precedence in the literature for comparing QENS measurements to other more "macroscopic" techniques, such as DSC, when studying the nature of transitions in polymer systems, especially the glass transition.[31−35] The reader is directed toward a discussion for this comparison by Ngai and

co-workers in the context of glass-forming liquids.[35] In general, the transitions observed in the elastic scattering, measured by QENS, are sensitive to changes in the mean square displacement, $\langle u^2 \rangle$ (i.e., the Debye−Waller factor), of the scattering particles. For glass forming liquids, it has been demonstrated that $\langle u^2 \rangle$ shows a sharp increase at the calorimetrically defined glass transition temperature, T_g.[32−35] Transitions observed in DSC and DMA are also manifested as a result of changes in the amplitude of motion (i.e., mean square displacement) of the molecules in the system. While these techniques probe longer time scales, they also probe larger length scales. Fixed window scans are probing fast relaxations at very short length scales on the order of angstroms. Therefore, any transitions in the amplitude of motion should be comparable to transitions observed with other techniques which are also sensitive to changes in the amplitude of molecular motions. In addition, as Angell[33] has pointed out, relaxation times can change by 8 orders of magnitude over a very narrow temperature range for typical fragile liquids. This argument was presented to explain why transitions in $\langle u^2 \rangle$ measured by QENS correspond closely with transitions determined by methods such as DSC. The elastic scattering intensity is related to the Debye−Waller factor and, therefore, is also subject to the same interpretation.[33]

By examining the elastic scattering intensity at higher Q values ($Q = 0.99$ Å^{-1}) as a function of temperature, Figure 4B, one observes an additional drop in the intensity at very low temperatures (approximately -150 °C). This transition is common among all three samples. It is useful to explain the origin of this transition considering the tetramethyl ammonium counterion because the hydrogens present are associated only with the methyl groups on this counterion. The origin for this decrease in the elastic scattering intensity can be attributed to methyl group rotations on the counterion. This type of transition has been observed for polymers and small molecules containing methyl groups and is well understood.[36−38] The larger counterions also show a similar, broader transition in this temperature regime. The deviation from the simple case of methyl rotors is due to the increasing level of complexity as the alkyl group becomes longer and includes −CH$_2$− groups. The molecular origin of the transition is likely due to complex rotational and librational motions of the alkyl "chain" of the counterion. This insight into the counterion dynamics will be discussed in detail below in context with the results obtained from dynamic scans and analysis of the elastic incoherent structure factor (EISF).

Variable Temperature Dynamic Scans. Further information regarding the dynamics of the counterions was obtained from measuring the quasielastic scattering in the energy range of ± 17 μeV and over a Q range of $0.25-1.75$ Å^{-1}. A typical dynamic structure factor ($S(Q,\omega)$) is shown in Figure 5 for TBA$^+$ Nafion at $Q = 0.99$ Å^{-1}. The measured $S(Q,\omega)$ was fit with a δ function convoluted with the instrument resolution function, a Lorentzian function, and a flat background. The Lorentzian function serves to account for the incoherent quasielastic component of the scattering and is given by

$$S_{inc}(Q,\omega) = \frac{1}{\pi}\frac{\Delta\omega(Q)}{\omega^2 + [\Delta\omega(Q)]^2} \quad (1)$$

where the half-width at half-maximum of the Lorentzian, $\Delta\omega(Q)$ (also represented as Γ (μeV)), is related to the diffusion of the hydrogen atoms in the sample.[39] These data have been analyzed by considering the diffusion of the hydrogen atoms within a sphere and a jump diffusion model. The continuous diffusion within a sphere model was developed by Volino and Dianoux[40] and has been used to describe the diffusion of water in Nafion membranes.[39,41] The scattering law for this model describes the diffusion of the scattering particle within a characteristic sphere of radius, R, and has been described in the literature.[39−41] While
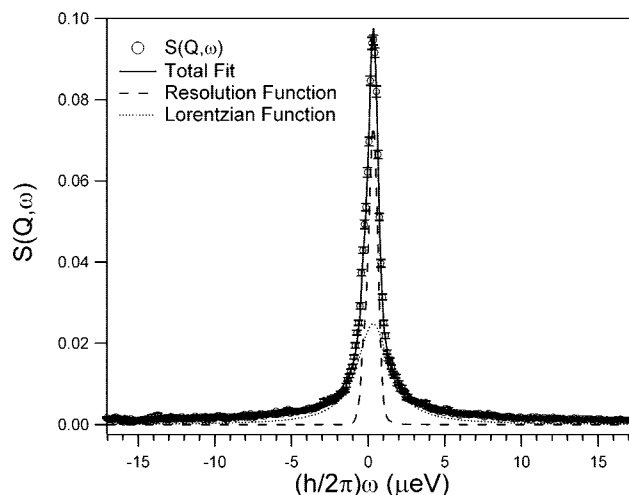

Figure 5. Example fitting of the dynamic structure factor, $S(Q,\omega)$.

this model takes into consideration the Lorentzian component of the QENS data and a single Lorentzian is enough to describe the scattering, it is likely that it is not sufficient to describe the intricacies of the counterion dynamics including methyl and methylene group rotations and the rotational motion of the entire counterion. In particular, it has been shown from the fixed-window data that at low temperatures the methyl and methylene group motions result in a decrease in the elastic intensity, which can lead to a broadening of the dynamic structure factor. However, the dynamic scans have been performed at high temperatures. The broadening observed can be attributed to different aspects of the counterion motion as it moves through the ion-hopping temperature. Therefore, when analyzing the diffusion of the hydrogen atoms within in a sphere, it is important to consider that this sphere may describe mobile portions of the counterion, or the entire counterion. In order to characterize the dynamic length scales and geometry of the counterion motions and to more specifically describe the motions occurring around the ion-hopping temperature, the elastic incoherent structure factor (EISF) was determined for each sample over a range of temperatures. The value of the EISF is defined as the ratio of the integrated intensity of the elastic peak to the total integrated intensity (i.e., quasielastic and elastic). In order to determine the spatial distribution of the diffusing hydrogen atoms, and indirectly the counterions, the spherical diffusion model was applied to the EISF using the following relationship[41]

$$\text{EISF}(Q) = \phi + (1 - \phi)\left(\frac{3j_1(QR)}{(QR)}\right)^2 \quad (2)$$

where ϕ accounts for the fraction of hydrogen atoms that are not diffusing within the time window of the experiment and $j_1(QR)$ is the first order Bessel function given by

$$j_1(QR) = \frac{\sin(QR)}{(QR)^2} - \frac{\cos(QR)}{(QR)} \quad (3)$$

where Q is the scattering vector and R is the radius of the sphere within which the dynamics occur.

The EISF for TMA$^+$ and TBA$^+$ at temperatures above and below their respective T_α's are shown in Figure 6, parts A and B. These data have been fit with eq 2, and the fits are represented by lines in Figure 6, parts A and B. From these data, we can conclude that at approximately $60-70$ °C below their respective α-relaxation temperatures, the counterion motion is very local and most of the scattering is elastic (i.e., the counterions do not have long-range mobility). This is confirmed by the values
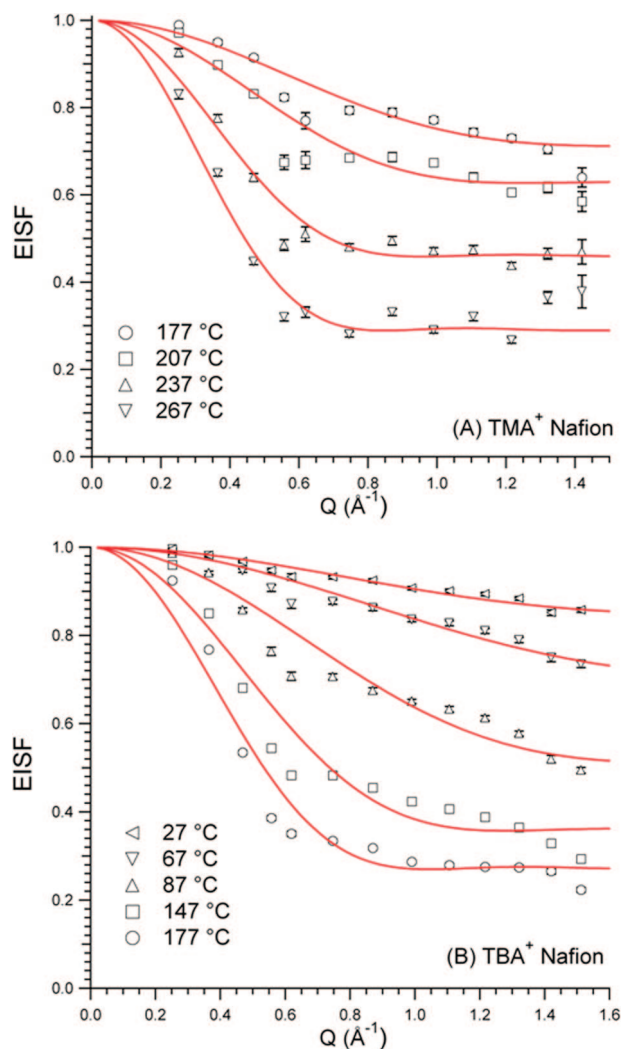
Figure 6. Elastic incoherent structure factor (EISF) for (A) TMA$^+$ Nafion at temperatures of (○) 177 °C, (□) 207 °C, (△) 237 °C, and (▽) 267 °C and for (B) TBA$^+$ Nafion at temperatures of (triangle pointing left) 27 °C, (▽) 67 °C, (△) 107 °C, (□) 147 °C, and (○) 177 °C. Solid lines are fits of eq 2 to the data.

of ϕ determined for each counterion below T_α. For TMA$^+$ at 177 °C the fraction of immobile hydrogens, ϕ, is approximately 0.71, while for TBA$^+$ at 27 °C ϕ is approximately 0.85. As the temperature is raised above the α-relaxation temperature, the scattering becomes dominated by the quasielastic component and the rapid decay in the EISF at low Q values is consistent with motions occurring over longer length scales than at lower temperatures. It should also be noted that when compared at the same temperature (177 °C) the fraction of immobile hydrogens is higher in the TMA$^+$ ($\phi \sim 0.71$) than for TBA$^+$ ($\phi \sim 0.27$), as indicated by the lower value of the EISF.

A fit of the EISF for TMA$^+$ Nafion at 177 °C (Figure 6A) results in a radius of 2.92 ± 0.3 Å, which correlates well with the reported crystallographic radius of the TMA$^+$ counterion (3.20, 3.47 Å).[42−44] Given the relative simplicity of the TMA$^+$ counterion it is important to consider these results together with the elastic scans described in Figure 4B. As discussed earlier, the decrease in the elastic scattering at low temperatures can be attributed to methyl group rotations. As the temperature is increased, the elastic scattering reaches a plateau before the second transition that has been attributed to ion-hopping. This plateau indicates that the quasielastic broadening due to methyl rotations has moved outside the resolution of the instrument. This, along with the excellent agreement between the charac-

teristic radius determined from the EISF at 177 °C and the reported radius of the TMA$^+$ counterion, seem to indicate that the motions at this temperature are due to counterion rotations. However, as the temperature increases, the radius increases to a value of 5.32 ± 0.2 Å at 267 °C. Atomistic simulations of Nafion by Devanathan and co-workers have shown that at low water concentrations, the distance between sulfur atoms is approximately 5 Å and is comparable to other values reported in the literature for similar systems.[45,46] This length scale is in excellent agreement with the characteristic radius of the sphere in which the dynamics occur as determined by modeling of the EISF for TMA$^+$ Nafion at temperatures above the ion-hopping temperature. From these data and the results obtained from modeling, a clear picture of the ion dynamics begins to emerge. At temperatures just below the ion-hopping temperature the TMA$^+$ counterion is rotating in place, but no long-range diffusion takes place. The absence of long-range diffusion is also supported by our earlier studies, in which no structural reorganization of oriented ion domains was observed below T_α.[19,20] At temperatures above the α-relaxation temperature, the hydrogen dynamics are occurring within a sphere that has a comparable radius to the distance between sulfur atoms. It can be concluded that at these temperatures the counterions can then effectively move between adjacent sulfonate groups, thus facilitating long-range diffusion. While these results have led to a general picture of the counterion dynamics, further high resolution QENS experiments must be carried out to refine our description of the dynamics.

A fit of the EISF for TBA$^+$ Nafion at 27 °C (Figure 6B) results in a radius of 2.12 ± 0.2 Å, which is much smaller than the reported crystallographic radius of the TBA$^+$ counterion (4.94 Å[47]). This suggests that at temperatures below the α-relaxation temperature the Lorentzian broadening is likely due to local motions of the butyl "arms" of the counterion. Due to the increased level of complexity in the TBA$^+$ counterion, this qualitative conclusion must be investigated further by performing high resolution QENS experiments and a much more sophisticated modeling. However, these results do give an indication that the motions are local and cannot facilitate long-range diffusion (i.e., hopping). The sphere increases to a size of 4.31 ± 0.2 Å at 177 °C, which is now comparable to the intersulfur distance determined by atomistic simulations, as discussed earlier. The counterions can then make the move to an adjacent sulfonate group. It should be noted that this radius is also comparable to the reported radius of the TBA$^+$ counterion. Therefore, it is likely that at temperatures above T_α the counterion is rotating and translating as it undergoes its long-range motion. This must be confirmed with further high-resolution experimentation.

By plotting the half-width at half-maximum ($\Gamma(\mu eV)$) versus Q^2 of the quasielastic component (Lorentzian) of $S(Q,\omega)$, the diffusive nature of the counterions has been ascertained. The data for both TMA$^+$ and TBA$^+$ Nafion at 267 and 177 °C, respectively, can be seen in Figure 7. The nonzero intercept of Γ at low Q values is indicative of spatially confined diffusion of the counterions[41,48] whereas the rise in Γ to an asymptotic value at high Q^2 values is consistent with random jump-diffusion within the confined spatial region.[39,41,48] These data have been analyzed using the following expression:

$$\Gamma\,(\mu eV) = \frac{\hbar}{\tau}(1 - \exp(-D_{jump}\tau Q^2)) + \frac{\hbar}{\tau_o} \tag{4}$$

Here $\hbar = 6.582 \times 10^{-16}$ eV·s, τ is the residence time between jumps measured in picoseconds (ps), D_{jump} is the jump diffusion coefficient, and Q is the scattering vector. The term $(\hbar)/(\tau_o)$ accounts for the nonzero intercept, is the residence time of the local confinement and can be used to determine
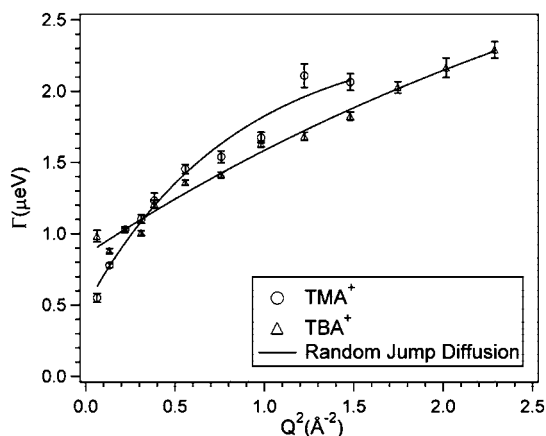
Figure 7. Half-width at half-maximum, Γ (μeV), of the Lorentzian component of $S(Q,\omega)$ versus Q^2. The solid line represents the fit of the random jump diffusion model (eq 4) to the data.

the local diffusion coefficient, D_{local}, using the following relationship

$$\Gamma_{Q \to 0} = 4.33 \frac{D_{local}}{R^2} \qquad (5)$$

where $\Gamma_{Q \to 0} = 1/\tau_o$, as determined by eq 4, and R is the characteristic radius of confinement determined by fitting the EISF with eq 2. In this application, local diffusion refers to the short-range mobility of the hydrogen atoms within the confinements of space surrounding the ionic species under the constraints of these short time-scale measurements.[48] The parameters for ion-hopping for TMA$^+$ at 267 °C and TBA$^+$ at 177 °C were determined from the data in Figure 7. The residence times between jumps for TMA$^+$ and TBA$^+$ are (411 $\pm$ 14) ps and (341 $\pm$ 29) ps, respectively and the jump diffusion coefficients, D_{jump}, were determined to be (4.39 $\pm$ 0.37) × 10^{-7} cm^2 s^{-1} for TMA$^+$ and (1.59 $\pm$ 0.1) × 10^{-7} cm^2 s^{-1} for TBA$^+$. The residence times and jump diffusion coefficients for the two counterion are of the same order of magnitude. It is important to note, however, that a direct comparison cannot be made because the results for each counterion were determined at different temperatures simply due to the dynamical behavior of the different systems. Also, it is likely that the dynamic components contributing to the broadening are somewhat different for the two counterions. According to Equation 5 the local diffusion coefficients, D_{local}, for the counterions are estimated to be 4.4 × 10^{-7} cm^2 s^{-1} and 4.8 × 10^{-7} cm^2 s^{-1} for TMA$^+$ and TBA$^+$, respectively. Work by Tierney and Register[11-13] has shown that the diffusion coefficients for the Na$^+$ and Li$^+$ cations in ethylene–methacrylate ionomer melts are on the order of 10^{-11} – 10^{-10} cm^2 s^{-1}, while Colby and co-workers[2] have shown that for polystyrene ionomers the diffusion coefficients for Na$^+$ and Rb$^+$ are on the order of 10^{-14} cm^2 s^{-1}. Both of these studies show considerably lower diffusion coefficients than those we have measured, however, it should be noted that the counterions used in these studies lead to very strong electrostatic interactions and overall lower chain mobilities. Rollet et al.[49,50] have studied the dynamics of TMA$^+$ ions in hydrated Nafion membranes. They found that the diffusion coefficients are on the order of 10^{-5} cm^2 s^{-1}, which is closer to the value measured in the work presented here. Of course, the dynamics measured in this study are slower since the membranes in this study are (1) dry and (2) in the melt.

As stated earlier, using QENS techniques for these particular systems allow one the unique advantage of probing the dynamics of the counterions themselves. However, it must be understood that while QENS probes the counterion dynamics, the polymer

chains are also undergoing dynamical processes and transitions. These motions include the main-chain of the polymer as well as the side-chains. Therefore, it is of fundamental importance that the results obtained and described above be interpreted in the context of earlier studies and what has already been demonstrated about the chain dynamics in these systems.[19,20,51,52] By correlating several techniques, a consistent and more detailed description of the dynamics begins to form. The data in this study show that at temperatures below the α-relaxation the counterion motions are local and that there is no long-range diffusion taking place. In earlier studies, it has also been shown that at temperatures below T_α, there is no relaxation of the ionic aggregates in oriented systems.[20] In order for large-scale morphological rearrangements to occur, the chains must be mobile enough to facilitate long-range motion. At temperatures comparable to T_α, the "ionomer peak" in SAXS has been shown to greatly diminish in intensity, and has been attributed to a more homogeneous spatial redistribution of the ions. Moreover, the chain motions that must occur with this spatial redistribution are noted to correlate very well with bulk relaxations measured by DMA. The current data, both from fixed-window and dynamic scans, show explicitly that long-range diffusion of the counterions begins to occur in the temperature range of T_α. Therefore, it can be concluded that the long-range diffusion of the counterions in this temperature range facilitate large-scale morphological rearrangements not possible at temperatures well below T_α. In addition, transitions measured in the side-chain dynamics from solid-state ^{19}F nuclear magnetic resonance (NMR) spectroscopy[19] clearly correlate with the transitions in the counterion dynamics measured here. Therefore, we can conclude that the motions of the counterions are dynamically coupled with the Nafion chains through the side-chains. These conclusions are consistent with earlier descriptions of the ion-hopping process for these materials.

Conclusions

The variable temperature small- and wide-angle X-ray scattering data show that the melting behavior of the PTFE-like crystallites are relatively unaffected by the choice of neutralizing counterion. In contrast, both the α- and β-relaxation temperatures are greatly affected by the choice of counterion. Therefore, it is readily apparent that the influence of the strength of the electrostatic interactions is the most important factor determining the segmental dynamics associated with the α-relaxation in such systems. Moreover, the use of QENS has proven to be a useful tool in studying the counterion dynamics in PFSI membranes. Through this study, we have been able to explicitly show that the α-relaxation in these materials is indeed linked to the onset of mobility of the counterions on the length-scale of 20−30 Å. To our knowledge, these data are the first direct *in situ* measure of the dynamics associated with the ion-hopping process in these ion-containing polymers. In addition, we have demonstrated that at temperatures below the α-relaxation the counterion motions are very local and that as the temperature is increased the amplitude of the motions approaches length-scales that facilitate ion-hopping between sulfonate groups. When considered together, the variable temperature X-ray scattering and the QENS studies not only serve to show that the α-relaxation is not related to the melting of PTFE-like crystallites in this material, but provide further fundamental understanding of the link between electrostatic interactions and the dynamics in perfluorosulfonate ionomers.

References and Notes

(1) Eisenberg, Adi; Kim, J.-S. *Introduction to Ionomers*; In John Wiley & Sons, Inc.: New York, 1998; pp 59−85.

(2) Colby, R. H.; Zheng, X.; Rafailovich, M. H.; Sokolov, J.; Peiffer, D. G.; Schwarz, S. A.; Strzhemechny, Y.; Nguyen, D. *Phys. Rev. Lett.* **1998**, *81*, 3876–3879.

(3) Eisenberg, A. *Macromolecules* **1970**, *3*, 147–154.

(4) Eisenberg, A.; Hird, B.; Moore, R. B. *Macromolecules* **1990**, *23*, 4098–4107.

(5) Greener, J.; Gillmor, J. R.; Daly, R. C. *Macromolecules* **1993**, *26*, 6416–6424.

(6) Han, S.-I.; Im, S. S.; Kim, D. K. *Polymer* **2003**, *44*, 7165–7173.

(7) Kim, J.-S.; Eisenberg, A. *J. Polym. Sci., Part B: Polym. Phys.* **1995**, *33*, 197–209.

(8) Kim, J.-S.; Jackman, R. J.; Eisenberg, A. *Macromolecules* **1994**, *27*, 2789–2803.

(9) Kim, J.-S.; Yoshikawa, K.; Eisenberg, A. *Macromolecules* **1994**, *27*, 6347–6356.

(10) Tant, M. R.; Mauritz, K. A.; Wilke, G. L., *Ionomers: Synthesis, Structure, Properties and Applications* Springer: Berlin, 1997; p 528.

(11) Tierney, N. K.; Register, R. A. *Macromolecules* **2002**, *35*, 6284–6290.

(12) Tierney, N. K.; Register, R. A. *Macromolecules* **2002**, *35*, 2358–2364.

(13) Tierney, N. K.; Register, R. A. *Macromolecules* **2003**, *36*, 1170–1177.

(14) Vanhoorne, P.; Register, R. A. *Macromolecules* **1996**, *29*, 598–604.

(15) Weiss, R. A.; Agarwai, P. K.; Lundberg, R. D. *J. Appl. Polym. Sci.* **1984**, *29*, 2719–2734.

(16) Weiss, R. A.; Fitzgerald, J. J.; Kim, D. *Macromolecules* **1991**, *24*, 1071–1076.

(17) Weiss, R. A.; Fitzgerald, J. J.; Kim, D. *Macromolecules* **1991**, *24*, 1064–1070.

(18) Brenner, D.; Oswald, A. A. Alkyl ammonium ionomers. US Patent 4,173,695, July 17, **1978**.

(19) Page, K. A.; Cable, K. M.; Moore, R. B. *Macromolecules* **2005**, *38*, 6472–6484.

(20) Page, K. A.; Landis, F. A.; Phillips, A. K.; Moore, R. B. *Macromolecules* **2006**, *39*, 3939–3946.

(21) Hird, B.; Eisenberg, A. *Macromolecules* **1992**, *25*, 6466–6474.

(22) Kim, J.-S.; Wu, G.; Eisenberg, A. *Macromolecules* **1994**, *27*, 814–824.

(23) Goswami, M.; Kumar, S. K.; Bhattacharya, A.; Douglas, J. F. *Macromolecules* **2007**, *40*, 4113–4118.

(24) Panagiotopoulos, A. Z. *Fluid Phase Equilib.* **1992**, *76*, 97–112.

(25) Yan, Q.; Pablo, J. J. d. *Phys. Rev. Lett.* **2002**, *88* (9), 1–4.

(26) Mauritz, K. A.; Moore, R. B. *Chem. Rev.* **2004**, *104* (10), 4535–4585.

(27) Meyer, A.; Dimeo, R. D.; Gehring, P. M.; Neumann, D. A. *Rev. Sci. Instrum.* **2003**, *74*, 2759–2777.

(28) http://www.ncnr.nist.gov/dave.

(29) Kline, S. R. *J. Appl. Crystallogr.* **2006**, *39*, 895–900.

(30) Cable, K. M.; Mauritz, K. A.; Moore, R. B. *J. Polym. Sci., Part B: Polym. Phys.* **1995**, *33*, 1065–1072.

(31) Colmenero, J.; Arbe, A. *Phys. Rev. B* **1998**, *57*, 13508–13513.

(32) Soles, C. L.; Douglas, J. F.; Wu, W.; Dimeo, R. M. *Macromolecules* **2003**, *36*, 373–379.

(33) Angell, C. A. *Science* **1995**, *267*, 1924–9135.

(34) Frick, B.; Richter, D. *Science* **1995**, *267*, 1939–1945.

(35) Ngai, K. L.; Bao, L.-R.; Yee, A. F.; Soles, C. L. *Phys. Rev. Lett.* **2001**, *87*, 1–4.

(36) Arrighi, V.; Ferguson, R.; Lechner, R. E.; Telling, M.; Triolo, A. *Physica B* **2001**, *301*, 35–43.

(37) Arrighi, V.; Higgins, J. S. *J. Chem. Soc., Faraday Trans.* **1997**, *93*, 1605–1612.

(38) Frick, B.; Fetters, L. J. *Macromolecules* **1994**, *27*, 974–980.

(39) Bee, M., *Quasielastic Neutron Scattering: Principles and Applications in Solid State Chemistry, Biology and Materials Science*; Adam Hilger: Philadelphia, PA, 1988.

(40) Volino, F.; Dianoux, A. J. *Mol. Phys.* **1980**, *41* (2), 271–279.

(41) Pivovar, A. M.; Pivovar, B. S. *J. Phys. Chem. B* **2005**, *109*, 785–793.

(42) Coetzee, J. F.; Cunningham, G. P. *J. Am. Chem. Soc.* **1965**, *87*, 2529–2534.

(43) Gill, D. S. *Electrochim. Acta* **1979**, *24*, 701–703.

(44) Robinson, R. A.; Stokes, R. H., *The Limiting Mobilities of Ions. In Electrolyte Solutions*, Butterworths Scientific Publications: London, 1955; pp 113−127.

(45) Devanathan, R.; Venkatnathan, A.; Dupuis, M. *J. Phys. Chem. B* **2007**, *111*, 8069–8079.

(46) Hristov, I. H.; Paddison, S. J.; Paul, R. *J. Phys. Chem. B* **2008**, *112*, 2937–2949.

(47) Barthel, J.; Gores, H.-J.; Schmeer, G.; Wachter, R. *Top. Curr. Chem.* **1983**, *111*, 33–144.

(48) Bellissent-Funal, M.-C.; Chen, S. H.; Zanotti, J.-M. *Phys. Rev. E* **1995**, *51*, 4558–4569.

(49) Rollet, A.-L.; Jardat, M.; Dufreche, J.-F.; Turq, P.; Canet, D. *J. Mol. Liq.* **2001**, *92*, 53–65.

(50) Rollet, A.-L.; Simonin, J.-P.; Turq, P.; Gebel, G.; Kahn, R.; Vandais, A.; Noel, J.-P.; Malveau, C.; Canet, D. *J. Phys. Chem. B* **2001**, *105*, 4503–4509.

(51) Osborn, S. J.; Hassan, M. K.; Divoux, G. M.; Rhoades, D. W.; Mauritz, K. A.; Moore, R. B. *Macromolecules* **2007**, *40*, 3886–3890.

(52) Page, K. A.; Jarrett, W.; Moore, R. B. *J. Polym. Sci., Part B: Polym. Phys.* **2007**, *45*, 2177–2186.